PHYSICAL REVIEW A **84**, 063835 (2011)

Coherent control of refractive index in far-detuned Λ systems

Chris O'Brien*
Department of Physics, Institute for Quantum Studies, Texas A&M University, College Station, Texas 77843-4242, USA

Petr M. Anisimov
Department of Physics and Astronomy, Hearne Institute for Theoretical Physics, Louisiana State University, Baton Rouge, Louisiana 70803, USA

Yuri Rostovtsev
Department of Physics, University of North Texas, Denton, Texas 76203, USA

Olga Kocharovskaya
Department of Physics, Institute for Quantum Studies, Texas A&M University, College Station, Texas 77843-4242, USA and Institute of Applied Physics, RAS, Nizhniy Novgorod, RU-603120 Russia
(Received 18 October 2011; published 15 December 2011)

Enhancement and control of the index of refraction in a mixture of two three-level atomic species that form a pair of far-detuned Λ schemes under two-photon resonance has been studied. We employ the density-matrix approach to properly take population relaxation into account and to describe the interaction of each Λ system with the electromagnetic fields. Both Λ systems are driven by a corresponding far-detuned coherent field at one atomic transition and are probed by the same weak field. In the dressed-state basis, it represents a superposition of effective two-level subsystems with the positions, widths, and amplitudes of the resonances controlled by the driving fields and allows for efficient control of the susceptibility of the total system; leading to refractive index (RI) enhancement with vanishing absorption in the absence of amplification. We analyze the experimental implementation of such a system in a cell of Rb atoms with a natural abundance of isotopes. An upper limit estimate of the RI enhancement is obtained.

DOI: 10.1103/PhysRevA.84.063835 PACS number(s): 42.50.Gy, 42.65.An

I. INTRODUCTION

Tightly focused laser radiation allows for the selective addressing of small regions of a medium. In microscopy, it is used to image tiny objects, such as biological cells, organic molecules, or nitrogen-vacancy centers in diamond. In lithography, it is used for the production of miniature semiconductor integral circuits. In information processing, it is used to provide multiple parallel optical channels. For all of these applications, a key issue is the spatial resolution that is defined by the minimum spot size the laser radiation can be focused to. This focal spot size fundamentally is limited by the wavelength of light in the medium λ, which depends on the refractive index (RI) n as follows: $\lambda = \lambda_{\text{vac}}/n$. Thus, high RI is very important for achieving high-spatial resolution in all of these applications. Materials with enhanced RI on demand also would be important for phase shifters, interferometers, and magnetic Faraday rotators.

Index of refraction characterizes the response of a medium to electromagnetic radiation, and hence, it is strongly enhanced near the atomic resonance. However, if a medium is in thermal equilibrium, the enhancement of RI near the atomic resonance is accompanied by an enhancement of absorption. Such that, when the maximal contribution from the atomic resonance to the RI is reached, the contribution to the absorption is the same. As a result, a 2π phase shift and an e-fold absorption take place at the same distance in a medium, which prevents the usage of the obtained RI in transmission experiments. In an inverted medium, high RI in the vicinity of the atomic resonance is accompanied by high gain. However, even higher gain is present at the exact resonance that makes such a system unstable and, again, nonsuitable for high-index applications.

A mixture of atomic species provides overlapping absorption and gain if the difference in resonance frequencies is on the scale of the linewidth and one of the atomic species is inverted. A proper overlap could result in a high RI with vanishing absorption for a weak field properly tuned between two atomic resonances. However, the difficulties associated with the practical implementation of such a combined system (finding proper species, providing for an even mixture, and providing population inversion for one species while avoiding spatial fluctuations in density and population exchange, etc.) would hardly be surmountable [1].

Here, we consider the idea to use coherent effects in a mixture of different species to induce strong and overlapping electromagnetic responses to provide high RI with vanishing absorption. The use of a coherent preparation of a medium for the elimination of absorption and index enhancement was pioneered by Scully [2], which was generalized further in Ref. [3] by including the density-dependent near-dipole-dipole interactions. A number of other three- and four-level schemes followed. They involved resonant driving at one or two atomic transitions and probing in a way that resonant enhancement of RI enhancement is accompanied by vanishing absorption [1]. It was expected that $\chi \sim 1$ without absorption would be

*cobrien.physics@gmail.com

possible in high-density ($N\lambda^3 \approx 50$) alkali metals but with an undesirable amplification region. Two schemes, however, a so-called double dark resonance and a degenerate double-Λ scheme allowed for the elimination of the gain region, although under a rather exotic and narrow range of parameters [4]. These developments led to a proof-of-principal experiment in Rb vapors, with a density of 10^{12} cm^{-3}, which showed RI enhancement with vanishing absorption. Although $N\lambda^3 \approx 1$ was achieved, the magnitude of index enhancement in this experiment was quite low, on the order of $\Delta n = 10^{-4}$ [5].

Recently, a scheme for coherent control and index enhancement was suggested by Yavuz [6]. This scheme is based on a resonant four-level system involving two Raman transitions optically pumped into the ground state and driven by two far off-resonant control fields forming two Λ systems with the same probe field. The dispersive and absorption characteristics in such a system as functions of two-photon detuning essentially interchange so that the maximum resonant RI is accompanied by vanishing absorption. Similar to the previous proposals involving resonant driving, the effect was attributed to interference and an index on the order of 10 for alkali-metal vapors with densities (10^{17} cm^{-3}) was predicted. Undesirable gain in the vicinity of vanishing absorption also was present.

We study a similar but simpler system. It represents itself as a mixture of two three-level atomic species, each driven by a corresponding far-detuned coherent field at one atomic transition and probed by the same weak field at an adjacent transition in the vicinity of two-photon resonance. This system was used in a proof-of-principal experiment that showed an enhancement of $\Delta n = 2.2 \times 10^{-7}$ [7]. In this paper, we analyze the physical mechanisms responsible for index enhancement in the case of far off-resonant driving and its limitations. We present a simple physically intuitive picture in the decaying dressed-state basis [8]. We then extend this analysis to include inhomogeneous broadening. In order to understand the limitations of RI enhancement in general and in this two-Λ scheme, we give a proper treatment of collisional broadening to show that any given mixture has a maximum possible index enhancement. We then give a detailed analysis of the proposed system in a cell of Rb atoms with natural abundances (72% ^{85}Rb and 28% ^{87}Rb) and compare it to the experimental results from Ref. [7]. An upper limit due to the dipole-dipole broadening at high atomic density of the RI enhancement in such a system is estimated as $\Delta n \simeq 0.2$.

II. THREE-LEVEL COHERENTLY DRIVEN SYSTEM: DENSITY-MATRIX FORMALISM

We consider a mixture of two atomic species with the density of atoms for each species N_{s1} and N_{s2} being free parameters. Each of them is represented as a three-level system, labeled by si $\in$ {s1,s2} with one excited state and two ground-state sublevels labeled $|a_i\rangle$, $|b_i\rangle$, and $|c_i\rangle$, correspondingly (see Fig. 1). The system, driven by a pair of coherent fields with frequencies ω_{si} and Rabi frequencies Ω_{si}, is probed by a weak field with frequency ω_{pr} and Rabi frequency α_{si}. The driving-field Rabi frequencies $\Omega_{si} = d_{si}^{ac} E_{si}/(2\hbar)$ are defined by the applied electric field E_{si} and the dipole moment of the transition d_{si}^{ac}. The Rabi frequencies of the probe field

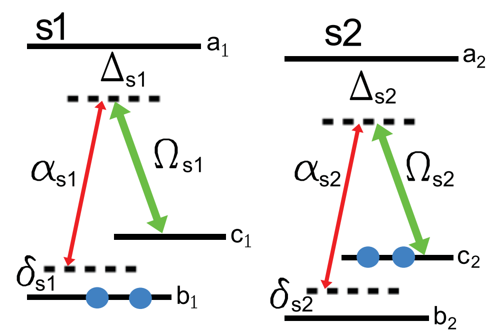

FIG. 1. (Color online) Mixture of two three-level Λ systems. The initially populated level is indicated by the dots.

$\alpha_{si} = d_{si}^{ab} E_{pr}/(2\hbar)$ in each system may be different because the dipole moment of the probed transition in the s1 system can be different from the dipole moment of the probed transition in the s2 system. All fields are far of-resonance from the atomic transitions so that one-photon contributions are negligible, implying $\Delta_{si} \gg \Omega_{si}$. The frequencies of the fields are chosen in such a way that they result in one two-photon transition in each three-level system involving one photon from the probe field and one photon from the corresponding driving field. So, each three-level system forms a Λ scheme with the same probe and corresponding driving field (see Fig. 1). Each three-level system is initially prepared in one of the two ground-state sublevels via optical pumping as indicated in Fig. 1. So, the first scheme exhibits two-photon absorption for the probe field while the second scheme provides two-photon gain.

The index of refraction and absorption coefficient can be found if the complex susceptibility is known. In our system, the total complex susceptibility is equal to the sum of individual contributions from each of the three-level systems. The complex susceptibility itself can be calculated if the optical coherence excited by a weak probe field is known as

$$\chi_{si} = \frac{3}{8\pi^2}\gamma_r^{si} N_{si}\lambda_{pr}^3 \frac{\sigma_{ab}^{si}}{\alpha_{si}}, \tag{1}$$

where $\gamma_r^{si} = \frac{4}{3}\frac{(d_{si}^{ab})^2}{4\pi\epsilon_0\hbar}\frac{(2\pi)^3}{\lambda_{pr}^3} = 8\pi^2(d_{si}^{ab})^2/(3\epsilon_0\hbar\lambda_{pr}^3)$ is the radiative decay rate of the probed transition, λ_{pr} is the wavelength of the probe, and σ_{ab}^{si} is the coherence of the probed transition.

We use density-matrix formalism and the rotating-wave approximation to calculate optical coherence induced by a weak probe field applied to the $a \leftrightarrow b$ transition in a three-level system driven off-resonance by a field applied to an adjacent transition $a \leftrightarrow c$. This formalism allows for including dephasing rates $\gamma_{\alpha\beta}^{si}$ at $\alpha \leftrightarrow \beta$ transitions, where $\{\alpha,\beta\} = \{a,b,c\}$. Similar to Ref. [6], we assume that driving fields do not disturb an initial population distribution, which implies either sufficiently short interaction time $t_{int}\Omega_{si}^2/\Delta_{si} \ll 1$ or sufficiently strong optical pumping through some additional levels (not indicated in Fig. 1).

The slowly varying amplitude of the optical coherence induced by a weak probe field $\alpha_{si} \ll \Omega_{si}$, γ_{ab}^{si} is found to be

$$\sigma_{ab}^{s1} = \frac{(\delta_{s1} - i\gamma_{cb}^{s1})\alpha_{s1}}{(\delta_{s1} + \Delta_{s1} - i\gamma_{ab}^{s1})(\delta_{s1} - i\gamma_{cb}^{s1}) - |\Omega_{s1}|^2} \tag{2}$$

for the s1 system presented in Fig. 1 (left), while for the s2 system presented in Fig. 1 (right), it is found to be

$$\sigma_{ab}^{s2} = -\frac{|\Omega_{s2}|^2\left(\Delta_{s2} + i\gamma_{ac}^{s2}\right)^{-1}\alpha_{s2}}{\left(\delta_{s2} + \Delta_{s2} - i\gamma_{ab}^{s2}\right)\left(\delta_{s2} - i\gamma_{cb}^{s2}\right) - |\Omega_{s2}|^2}. \quad (3)$$

In these equations, we introduced the following parameters for the si system: $\Delta_{si} = \omega_{ab}^{si} - \omega_{cb}^{si} - \omega_{si}$ and $\delta_{si} = \omega_{si} + \omega_{cb}^{si} - \omega_{pr}$ are the one- and the two-photon detunings for the si-drive field, respectively.

Finally, we can write down the expression for complex susceptibility of the system,

$$\chi(\omega_{pr}) = \frac{3\lambda_{pr}^3}{8\pi^2}\left(\frac{N_{s1}\gamma_r^{s1}\left(\delta_{s1} - i\gamma_{cb}^{s1}\right)}{\left(\delta_{s1} + \Delta_{s1} - i\gamma_{ab}^{s1}\right)\left(\delta_{s1} - i\gamma_{cb}^{s1}\right) - |\Omega_{s1}|^2} - \frac{N_{s2}\gamma_r^{s2}|\Omega_{s2}|^2\left(\Delta_{s2} + i\gamma_{ac}^{s2}\right)^{-1}}{\left(\delta_{s2} + \Delta_{s2} - i\gamma_{ab}^{s2}\right)\left(\delta_{s2} - i\gamma_{cb}^{s2}\right) - |\Omega_{s2}|^2}\right). \quad (4)$$

In the following sections, individual contributions are discussed, and physical insights are given.

III. DRESSED-STATE ANALYSIS: EFFECTIVE TWO-LEVEL SYSTEMS

The slowly varying amplitude of the optical coherence induced by a weak probe field in a Λ configuration is inversely proportional to a quadratic polynomial in terms of the two-photon detuning δ_{si}. Zeros of this polynomial correspond to the two main contributions to the optical coherence. Expanding the coherence into Lorentzians defined by each zero gives the decaying dressed states as previously discussed in Ref. [8].

For the case of a far-detuned driving field, $\Delta_{si} \gg \Omega_{si}, \gamma_{ab}^{si}, \gamma_{cb}^{si}$, these resonance contributions are far detuned as well and are associated with one- and two-photon resonances. This clearly is seen for s1 after expanding Eq. (2) in terms of the small parameter $\xi_{si} = |\Omega_{si}|^2/\Delta_{si}^2$,

$$\sigma_{ab}^{s1} = \frac{\alpha_{s1}(1-\xi_{s1})}{\delta_{s1} - \Delta_{s1}(1-\xi_{s1}) - i\left[\gamma_{ab}^{s1}(1-\xi_{s1}) + \gamma_{cb}^{s1}\xi_{s1}\right]} + \frac{\alpha_{s1}\xi_{s1}}{\delta_{s1} - \Delta_{s1}\xi_{s1} - i\left[\gamma_{cb}^{s1}(1-\xi_{s1}) + \gamma_{ab}^{s1}\xi_{s1}\right]}. \quad (5)$$

If $\Delta_{s2} \gg \gamma_{ac}^{s2}$ as well, a similar expression can be found for s2 with the exception that the two-photon amplitude is now negative and, therefore, provides gain due to the population in level $|c_2\rangle$; while the one-photon amplitude is different since the feature would no longer be present in the absence of a control field,

$$\sigma_{ab}^{s2} = \frac{\alpha_{s2}\xi_{s2}}{\delta_{s2} - \Delta_{s2}(1-\xi_{s2}) - i\left[\gamma_{ab}^{s2}(1-\xi_{s2}) + \gamma_{cb}^{s2}\xi_{s1}\right]} + \frac{-\alpha_{s2}\xi_{s2}}{\delta_{s2} - \Delta_{s2}\xi_{s2} - i\left[\gamma_{cb}^{s2}(1-\xi_{s2}) + \gamma_{ab}^{s2}\xi_{s2}\right]}. \quad (6)$$

Furthermore, our probe field ω_{pr} is tuned to the vicinity of two-photon resonance ($\delta_{si} \ll \Delta_{si}$), therefore, the contribution from the one-photon resonance of the second system can always be neglected, while the one-photon contribution of the first system can be neglected when $\gamma_{ab}^{s1}/\Delta_{s1} \ll \xi_{s1}$.

When the low-frequency coherence decays slower than the optical one $\gamma_{ab}^{si} \gg \gamma_{cb}^{si}$, the contribution from the two-photon resonance nearly can be as large as the contribution from the one-photon resonance. This would simply require $\xi_{si} \geqslant \gamma_{cb}^{si}/\gamma_{ab}^{si}$. Hence, both of our three-level schemes behave as effective two-level schemes with susceptibilities on the same order as the ones for the original transition. The presence of the drive fields allow for the control of the strength, width, and position of the resonances. This, in turn, leads to the manipulation of the atomic responses of the individual systems (see Fig. 2). We will use this flexibility combined with appropriate mixing of the species to obtain enhanced RI without absorption.

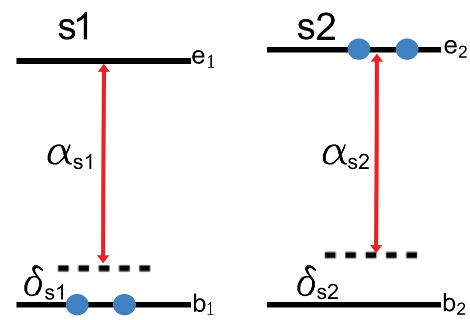

FIG. 2. (Color online) An equivalent representation of a mixture of two three-level subsystems driven by coherent off-resonant fields.

At first, we take an approach similar to Ref. [6]. It is based on the absorption and amplification resonances having the same magnitude and width while being separated by the full width at half maximum (FWHM). This arrangement results in the absorption being compensated by nearby gain. Furthermore, at the point of no absorption, the maximum (minimum) of the real part of the complex susceptibility associated with the absorption resonance adds up with the maximum (minimum) of the real part of the complex susceptibility associated with the gain resonance. We demonstrate this (see Fig. 3) by calculating the atomic response from a mixture of two three-level subsystems for the case of $\xi_{si} \approx \gamma_{cb}^{si}/\gamma_{ab}^{si}$. Numerical values

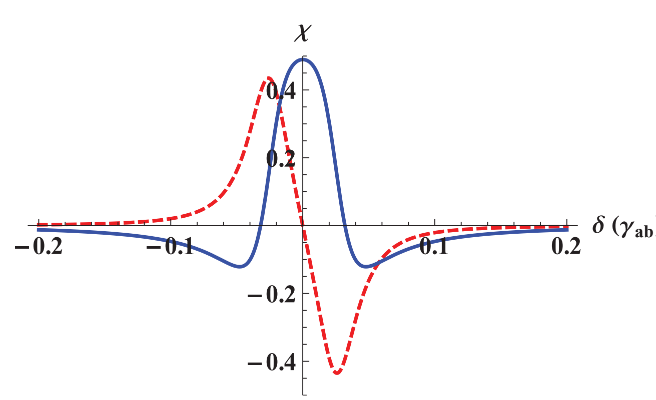

FIG. 3. (Color online) Combined real (solid) and imaginary (dashed) parts of the susceptibility from two three-level systems where the x axis is normalized to $\gamma_{ab}^{s1} = \gamma_{ab}^{s2} = \gamma_{ab}$ and the y axis is normalized to $\eta = 3N_{s1}\lambda_{pr}^3\gamma_r^{s1}/(8\pi^2) = 3N_{s2}\lambda_{pr}^3\gamma_r^{s2}/(8\pi^2) = 1$ with $\Omega_{s1} = \Omega_{s2} = 2\gamma_{ab}$, $\Delta_{s1} = \Delta_{s2} = 20\gamma_{ab}$, and $\gamma_{cb}^{s1} = \gamma_{cb}^{s2} = 0.016\gamma_{ab}$. Resonances have equal strength and width but are shifted by FWHM. The obtained maximum at zero absorption is 0.5η.

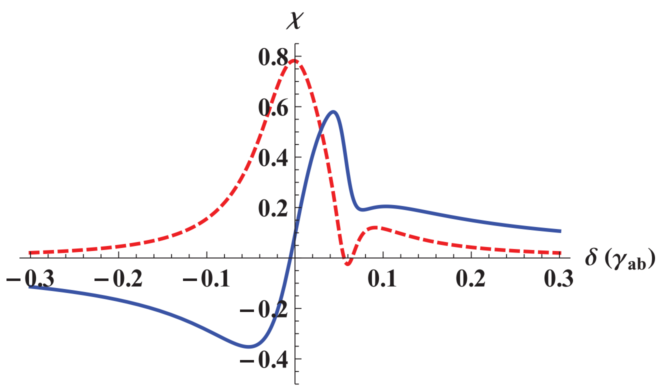

FIG. 4. (Color online) Combined real (solid) and imaginary (dashed) parts of the susceptibility from two three-level systems. With $\Omega_{s1} = 4\gamma_{ab}$ and $\Omega_{s2} = 1.5\gamma_{ab}$ and all other parameters, the same as in Fig. 3. Amplification is weaker and is narrower than absorption. The relative shift is adjusted to get zero absorption and no gain. The obtained maximum at zero absorption is 0.33η.

of the parameters used are listed in the caption to the figure. Although this arrangement provides a high value of RI with no absorption, the disadvantage of such an approach can easily be seen in Fig. 3. Namely, noncompensated gain is present in close proximity to the point of enhanced RI. In order to avoid undesirable gain in the system, we suggest an alternative to the previously outlined approach. This is performed at the expense of a reduced enhancement in the RI. In this approach, a narrower amplification resonance is superimposed on top of a broader absorption resonance as previously suggested in Ref. [9]. The amplification resonance is positioned at the maximum of the real part of the complex susceptibility associated with the absorption resonance. The magnitude of the amplification resonance is chosen to compensate present absorption in the narrow region without providing gain. For such an arrangement, the amplification resonance provides no contribution to the RI enhancement at the point of no absorption. In order to demonstrate the approach, we present the atomic response of the mixture of two three-level systems in Fig. 4 for the parameters listed in the caption of the figure.

As an alternative to the species providing absorption, instead of a three-level system, we can just use a two-level atom that provides absorption. This is natural since we want the absorption feature to be both stronger and wider than the gain feature, and the effective two-level transition always is weaker and narrower than the original two-level transition. The only reason this is not always ideal is that it eliminates one of the knobs we can turn to match the transitions. Since the same probe field addresses both the two-level absorption transition and the far-detuned Λ scheme, it is necessary for the one-photon detuning of our gain system to match the difference in transition frequencies between the two transitions, i.e., $\Delta_{s2} \approx \omega_{ab}^{s2} - \omega_{ab}^{s1}$. Since we also need the one-photon detuning to be much larger than the linewidth of the optical transition, then for this implementation to be appropriate, we need $\omega_{ab}^{s2} - \omega_{ab}^{s1} \gg \gamma_{ab}^{si}$, but since the control-field Rabi frequency is proportional to Δ_{s2}, we need the difference to be small enough such that a reasonably sized control-field Rabi frequency can still satisfy $\xi_{s2} > \gamma_{cb}^{s2}/\gamma_{ab}^{s2}$. If either of these conditions is not satisfied, we are forced to use a far-detuned Λ scheme for both absorption and gain.

So far, we have been discussing the atomic response of a pair of three-level systems. This discussion has demonstrated that RI with no absorption is possible to obtain in the presented system. The maximum value for the RI is limited by the value for the original two-level system with the main difference that it is achieved with no absorption or amplification in the vicinity of maximum value. Therefore, in order to get the maximum value of RI enhancement, the original two-level resonant susceptibility has to be maximized by choosing an appropriately high concentration.

IV. EFFECT OF INHOMOGENEOUS BROADENING

In the previous section, it has been shown that the two-photon resonant feature is equivalent to an effective two-level atomic system with the amplitude, frequency, and width of the transition controlled by the driving field. Furthermore, the electromagnetic response of this effective system can be as strong as the resonant response of an actual two-level system. This is shown under the assumption of homogeneous broadening, when values of the Rabi frequency Ω_{si} and one-photon detuning Δ_{si} are well defined by the intensity and frequency of the driving field. In the case of inhomogeneous broadening of the probed transition, the frequency of the driving field defines only the mean value of one-photon detuning Δ_0 while variance is defined by inhomogeneous broadening. Namely, $\Delta_{si} = \Delta_0 + \Delta_{inh}$ with $\langle\Delta_{inh}^2\rangle - \langle\Delta_{inh}\rangle^2 = (\gamma_{ab}^{inh})^2$ where $\langle\cdots\rangle$ is averaging over the inhomogeneous profile. For the case of inhomogeneous broadening of the $c \leftrightarrow b$ transition, we only have a mean value of the two-photon detuning δ_0 while the varying detuning is given by $\delta_{si} = \delta_0 + \delta_{inh}$ with $\langle\delta_{inh}^2\rangle - \langle\delta_{inh}\rangle^2 = (\gamma_{cb}^{inh})^2$. Therefore, the two-photon transition probability, frequency, and width also are not well-defined.

The inhomogeneous profile in both solids and gases will be Gaussian, but in order to easily deal with the analytic expressions, we will approximate with a Lorentzian profile. If we start with the coherence given by Eqs. (2) or (3), we can integrate over the Lorentzian distributions of the one- and two-photon detunings,

$$\sigma_{ab}^{inh} = \int_{-\infty}^{\infty} d\Delta_{inh} \frac{\gamma_{ab}^{inh}/\pi}{\Delta_{inh}^2 + \left(\gamma_{ab}^{inh}\right)^2} \times \int_{-\infty}^{\infty} d\delta_{inh} \frac{\gamma_{cb}^{inh}/\pi}{\delta_{inh}^2 + \left(\gamma_{cb}^{inh}\right)^2} \sigma_{ab}(\Delta_{inh},\delta_{inh}). \quad (7)$$

In the limit examined in Sec. III, $\Delta_0 > \gamma_{ab}^{si},\gamma_{cb}^{si},\Omega_{si}$, these integrals can be solved analytically, which shows that the inhomogeneous profile can be taken into consideration in all the equations, which we derive simply by replacing the homogeneous linewidths with the total linewidth that includes the inhomogeneous broadening, i.e., $\gamma_{ab}^{si} \to \gamma_{ab}^{si} + \gamma_{ab}^{inh} + \gamma_{cb}^{inh}$ and $\gamma_{cb}^{si} \to \gamma_{cb}^{si} + \gamma_{cb}^{inh}$, except for system 2 where we also have to replace $\gamma_{ac}^{si} \to \gamma_{ac}^{si} - \gamma_{ab}^{inh}$. It is important to keep in mind that this is not a change in the linewidth of the $a \leftrightarrow c$ transition, just in how the decoherence of this transition comes into Eq. (3), and Eq. (6) is still valid when $\Delta_{s2} \gg \gamma_{ab}^{inh}$.

Therefore, one can see that the quantity that matters is the total linewidth. Thus, all previous discussions could be repeated here with $\gamma_{ab}^{\rm si}$ being replaced by the total linewidth. This makes our final statement sound as follows: electromagnetic response of an effective two-level system, which is fully controlled by a weak off-resonant driving field, is as strong as the resonant electromagnetic response of the actual two-level $a \leftrightarrow b$ transition without a driving field being present regardless of the broadening if the total linewidth is considered. Broadening of the transition beyond the natural linewidth weakens the response of the system as well as the intensity required to reach the maximal obtainable value.

V. COLLISIONAL BROADENING

Electromagnetic response of an atomic system can be increased by improving the $\gamma_{\rm r}^{\rm si}/\gamma_{ab}^{\rm si}$ ratio and by having more atoms per cubic wavelength $N_{\rm si}\lambda_{\rm pr}^3$. The second approach seems to be the easiest, but it leads to a decrease in the aforementioned ratio due to atomic interaction in dense media. The large estimates for achievable RIs in previous papers were due to not considering the effect of increasing density on the ratio $\gamma_{\rm r}^{\rm si}/\gamma_{ab}^{\rm si}$. According to Lewis [10], the collisional contribution to the linewidth is proportional to concentration N, namely, the half width at half maximum (HWHM), which is as follows:

$$\Gamma_{\rm coll}^{\rm si} \simeq f_{\rm si} c r_e \lambda_{\rm pr} N \sqrt{g_g^{\rm si}/g_e^{\rm si}}, \tag{8}$$

with $g_g^{\rm si}$ and $g_e^{\rm si}$ as the degeneracies of the ground and excited states, respectively, r_e is the classical radius of the electron, and $f_{\rm si}$ is the oscillator strength of the transition. This broadening comes from the resonant dipole-dipole interaction between induced optical dipoles, where, in Eq. (8), we have used the total population $N = N_{\rm s1} + N_{\rm s2}$ since atoms with similar transition frequencies are identical with regard to collisions. For example, take the ^{85}Rb D_1 line; Eq. (8) gives $\Gamma_{\rm coll} = 0.365 \times 10^{-13} N$ MHz cm^3 and Ref. [11] measures the self-broadening as $\Gamma_{\rm coll} = 0.375(\pm 0.12) \times 10^{-13} N$ MHz cm^3, therefore, this equation gives an accurate estimate.

For a Doppler broadened gas, the inhomogeneous broadening additively contributes to the total broadening in our scheme. The Doppler contribution is given by the HWHM of the Maxwell distribution for each species,

$$\Gamma_D^{\rm si} = \sqrt{\frac{2kT \ \ln 2}{m_{\rm si} c^2}}\,\omega_0, \tag{9}$$

where k is the Boltzmann constant, T is the absolute temperature of the gas, $m_{\rm si}$ is the mass of the atomic species, c is the speed of light, and $\omega_0 = 2\pi c/\lambda_{\rm pr}$ is the transition frequency.

In a hot-gas cell, the density is determined by the temperature of the cell, so both the inhomogeneous Doppler broadening and the homogeneous collisional broadening are dependent on the density. Since we want a large resonant RI, we are interested in high gas densities. The susceptibility of the effective two-level system always is constrained by the original two-level susceptibility of the $a \leftrightarrow b$ transition, which is given by

$$\chi_{\rm max}^{\rm si} = \frac{3}{8\pi^2}\frac{N_{\rm si}\lambda_{\rm pr}^3\gamma_{\rm r}^{\rm si}}{0.5\gamma_{\rm r}^{\rm si} + \Gamma_D^{\rm si} + \Gamma_{\rm coll}^{\rm si}}. \tag{10}$$

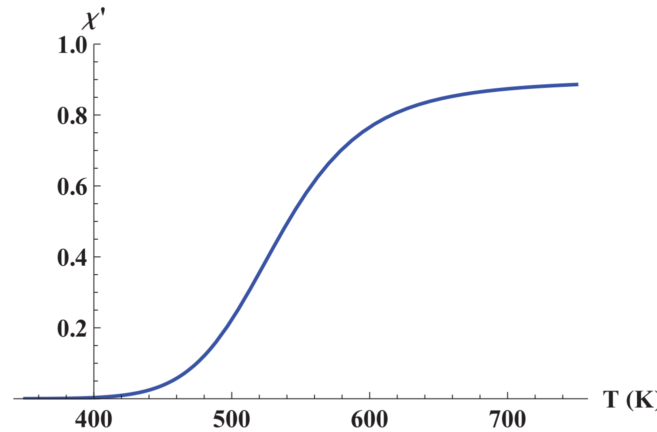

FIG. 5. (Color online) The peak real part of the susceptibility for the D_2 line of ^{85}Rb as a function of absolute temperature.

Since the linewidth and total atomic response grow linearly with concentration, eventually with increased density, the susceptibility will saturate. This happens when $\Gamma_{\rm coll}^{\rm si} \gg 0.5\gamma_{\rm r}^{\rm si} + \Gamma_D^{\rm si}$.

Consider the D_2 line of ^{85}Rb with $\Gamma_{\rm coll} = 0.515 \times 10^{-13} N$ cm^3 MHz. When the collisional broadening becomes much larger than the other broadening terms, the two-level susceptibility saturates at 750 K or a density of $N \approx 6 \times 10^{17}$ cm^{-3} (see Fig. 5). This leads to a maximum real part of the resonant susceptibility of 0.885 or a RI of 1.37. Therefore, there is no way to enhance the RI of rubidium past $\Delta n = 0.4$.

VI. RATIO OF HYPERFINE COHERENCE TO OPTICAL COHERENCE

The main limitation for our effective two-level transition to have as high a susceptibility as the original transition is the need for a strong control-field Rabi frequency $|\Omega_{\rm si}|^2 > \Delta_{\rm si}^2 \gamma_{cb}^{\rm si}/\gamma_{ab}^{\rm si}$. Therefore, to minimize the needed intensity, we need as small a hyperfine decoherence as possible, $\gamma_{cb}^{\rm si} \ll \gamma_{ab}^{\rm si}$.

At low densities, the main contribution to the hyperfine decoherence is due to time of flight in our control beams since, as atoms leave the interaction region, the coherence decreases. This decoherence rate can be described as [12]

$$\Gamma_{\rm TF}^{\rm si} = \frac{\sqrt{2}\,\ln 2}{2\pi d}\sqrt{\frac{2kT}{m}}, \tag{11}$$

where d is the $1/e$ diameter of the beam. While at high densities, the main contribution to the hyperfine broadening is the decay of hyperfine population due to spin-exchange collisions between two atoms. This self-broadening, such as collisional broadening, is linearly proportional to the density. For example, for ^{85}Rb, we can estimate the decoherence as $\Gamma_{\rm SB}^{\rm si} = 2\pi \times 2.83 \times 10^{-16} N$ MHz [13].

The time-of-flight decoherence can be decreased by including a neutral buffer gas. Then, as our atomic species is leaving the beam area, it repeatedly collides with the buffer-gas atoms leading to a longer path length in the beam. With the

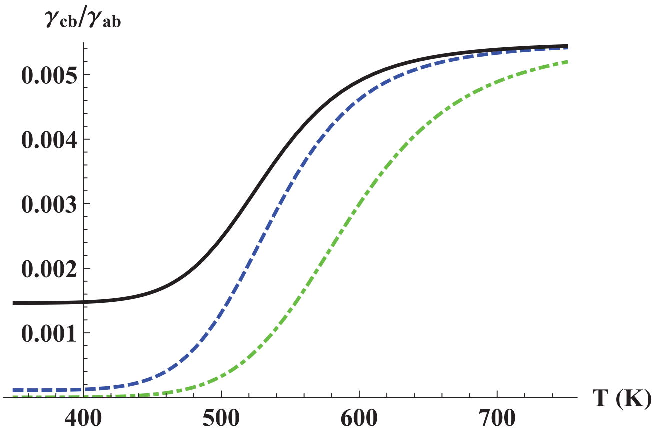

FIG. 6. (Color online) The ratio of hyperfine-to-optical decoherence rates for the D_2 line of ^{85}Rb plotted as a function of temperature for the case where there is no buffer gas (solid), with a neon buffer gas at 10 Torr (dashed line), and at 300 Torr (dot-dashed line).

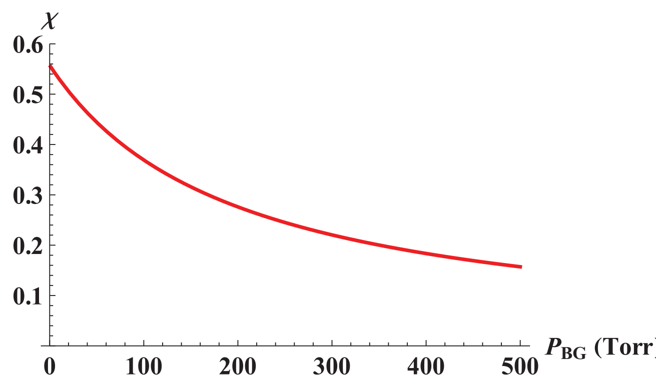

FIG. 7. (Color online) The maximum real part of the two-level susceptibility for the Rb D_2 line plotted as a function of the buffer-gas pressure. Plotted at a temperature of 550 K.

background gas, the time-of-flight decoherence rate given by Eq. (11) will be replaced by [10]

$$\Gamma_{TF}^{si} = \left(\frac{4.81}{d}\right)^2 D_0 \frac{P_0}{P_{BG}}, \qquad (12)$$

where D_0 is the diffusion coefficient measured at a reference pressure of P_0 and P_{BG} is the buffer-gas pressure. The buffer gas also will broaden both transitions due to collisional broadening, while even at high buffer pressures, collisions with the buffer gas only will have a negligible effect on γ_{cb}^{si} but will have a noticeable addition to the optical coherence that will scale linearly with buffer-gas pressure. At high buffer-gas pressures, this effect significantly can reduce the maximum susceptibility possible.

For example, consider the Rb D_2 line; we can express the buffer-gas contribution to the collisional decoherence as $\Gamma_{BG}^{si} = 2\pi \times (4.735\ \text{MHz/Torr}) \times P_{BG}$ with P_{BG} measured in Torr [14]. $D_0 = 0.21\ \text{cm}^2/\text{s}$ for $P_0 = 760$ Torr [15], giving for $d = 1$ mm, $\Gamma_{TF}^{si} = 2\pi \times 0.369\ \text{MHz Torr}/P_{BG}$. For this case, the effect of the buffer gas on the decoherence ratio is shown in Fig. 6. Since the collisional broadening increases as the buffer-gas pressure is increased, for maximum RI enhancement, it is better to use a low-pressure buffer gas as can be seen in Fig. 7.

VII. IMPLEMENTATION IN GAS

Alkali metals, such as lithium, rubidium, and potassium have been good test systems for demonstrating many coherent effects. To demonstrate RI enhancement, one needs to find two transitions with frequency differences in the megahertz to gigahertz range. This is possible if a mixture of isotopes is considered. Of the three alkali-metal atoms with stable isotopes, however, only rubidium has a comparable ratio of naturally occurring isotopes (28% of ^{87}Rb and 72% of ^{85}Rb) and large enough hyperfine splitting. Thus, as a physical example, let us consider a mixture of Rb vapors at natural abundances.

Rb atoms have two suitable transitions called D_1 at 794.8 nm and D_2 at 780.2 nm. The D_1 and D_2 transitions have common ground levels and differ in the excited states. The excited-level structure for the D_1 and D_2 transitions has a separation less than 0.8 GHz, thus, for one-photon detunings much larger than this separation, the value of an effective far-detuned dipole moment can be used. Numerical values for π-polarized light are $1.727ea_0$ and $2.44ea_0$ for D_1 and D_2 transitions correspondingly. A stronger dipole moment guarantees a stronger atomic response and, therefore, larger susceptibilities. A stronger dipole moment also implies a lower intensity requirement for the control fields to reach the needed Rabi frequency. Therefore, the D_2 transition seems to be the optimal choice from all accounts. The natural linewidth of the Rb D_2 absorption line is $2\pi \times 6.067$ MHz, although the radiative decay rate is $2\pi \times 5.12$ MHz.

In order to implement RI enhancement with vanishing absorption while maintaining no nearby regions of gain in a Rb gas, it is necessary to implement system 1 in ^{85}Rb and system 2 in ^{87}Rb. Since at natural abundances, the density of ^{85}Rb is nearly three times larger than ^{87}Rb, and we need the effective-absorption transition to be stronger than the effective-gain transition. This choice also determines the one-photon detuning for system 1 since, if we want the same probe field to address both transitions, then the difference in transition frequencies $\omega_{ab}(^{87}\text{Rb}) - \omega_{ab}(^{85}\text{Rb}) = 2\pi \times 0.39$ GHz determines the difference in one-photon detunings. The ground state of Rb has two hyperfine levels separated by $2\pi \times 3.036$ and $2\pi \times 6.835$ GHz for the ^{85}Rb and ^{87}Rb isotopes, respectively. We assume that the probe field is applied to the lower of the two hyperfine levels and the control fields are applied to the upper levels. First, it tells us that we need $\Delta_{si} > 2\pi \times 8$ GHz in order to avoid one-photon resonance, therefore, we take $\Delta_{s2} = 2\pi \times 10$ GHz, implying $\Delta_{s1} = 2\pi \times 10.385$ GHz.

Except for the transition frequencies, all other properties of interest for ^{85}Rb and ^{87}Rb, including the dipole moments and the decoherence rates, are essentially the same when the slight mass difference is neglected. The decoherence rate of the optical transition has four contributions: $\gamma_{ab}^{si} = 0.5\gamma_r^{si} + \Gamma_{coll}^{si} + \Gamma_D^{si} + \Gamma_{BG}^{si}$. The radiative decay rate fairly is unaffected by density and is given by $\gamma_r^{si} = 2\pi \times 5.12$ MHz. As discussed in Sec. V, we can take the ideal density for

Rb to be $N = 6 \times 10^{17}$ cm^{-3}; unfortunately, at this density. $\gamma_{ab}^{si} = \gamma_{ac}^{si} = 197$ GHz, which violates our condition to avoid the one-photon absorption of $\Delta_{si} \gg \gamma_{ab}^{si}, \gamma_{ac}^{si}$ since having such a large one-photon detuning would lead to an unachievable Rabi frequency.

Say, for our control fields, we are limited to focusing a 100-mW beam into a diameter of 1 mm, this would give us Rabi frequencies of $2\pi \times 150$ MHz, so we take $\Omega_1 = 2\pi \times 150$ and $\Omega_2 = 2\pi \times 135$ MHz, implying that the maximum control-field ratio ξ_{si} we can achieve is 2.25×10^{-4}. The decoherence ratio is equal to this ξ_{si} at a temperature of $T = 450$ K or a density of $N = 3.3 \times 10^{14}$ cm^{-3}, so, at natural abundances, we have $N_{s1} = 0.72$ and $N_{s2} = 0.28$ N. For a fixed ξ_{si}, a lower buffer-gas pressure is better, so we take $P_{BG} = 10$ Torr. This buffer gas adds $2\pi \times 47$ MHz to the optical decoherence, and the time-of-flight broadening is $\Gamma_{hyp,BG}^{si} = 2\pi \times 37$ kHz. At this density, the hyperfine self-broadening is $\Gamma_{hf,self}^{si} = 2\pi \times 93$ kHz, so $\gamma_{cb}^{si} = 2\pi \times 130$ kHz. The collisional broadening is $\Gamma_{coll}^{si} = 2\pi \times 17$ MHz, and the Doppler broadening is $\Gamma_D^{si} = 2\pi \times 315$ MHz, therefore, $\gamma_{ab}^{si} = 2\pi \times 382$ MHz, giving a ratio of $\gamma_{cb}^{si}/\gamma_{ab}^{si} = 3.4 \times 10^{-4}$.

With these values for the detunings and Rabi frequencies, the susceptibility is plotted in Fig. 8. There is a particular frequency where we have vanishing absorption and a significant resonant susceptibility Re $\chi = 0.0095$. At the same time, we have no regions of nearby gain so that the probe field remains stable at that frequency. Therefore, in a hot Rb gas, we have a maximum RI enhancement on the order of $\Delta n \approx 4.7 \times 10^{-3}$.

When it is possible to use strong control fields, we can achieve the maximum possible susceptibility increase. Consider focusing a 10-W beam into a 1-mm diameter, then the Rabi frequencies are $\Omega_{s1} = \Omega_{s2} = 2\pi \times 1.5$ GHz. This allows us to use larger one-photon detunings to $\Delta_{s1} = 2\pi \times 20$ and $\Delta_{s2} = 2\pi \times 20.27$ GHz, which gives $\xi_{s1} = 0.0055$, allowing for a higher ratio of $\gamma_{ab}^{si}/\gamma_{cb}^{si}$. Taking $T = 600$ K, gives us $N = 4 \times 10^{16}$ cm^{-3}, which leads to $\gamma_{ab}^{si} = 2\pi \times 4.667$ GHz and $\gamma_{cb}^{si} = 2\pi \times 71$ MHz. Then, the change in index is $\Delta n = 0.18$, as shown in Fig. 9.

Since the isotope shift for rubidium $\omega_{ab}(^{87}\text{Rb}) - \omega_{ab}(^{85}\text{Rb}) = 2\pi \times 0.39$ GHz is smaller than our linewidths, it would not be possible to use the two-level transition rather than the effective two-level transition for absorption as discussed at the end of Sec. III. To implement such a system, we would need isotope shifts on the order of 10 GHz, which only are possible when the masses of the two isotopes are significantly different compared to the isotope mass. For example, such a system could be implemented in lithium.

VIII. EXPERIMENTAL REALIZATION

A proof-of-principal experiment to demonstrate resonant enhancement of RI in hot Rb gas was performed by Yavuz [7]. The same two Λ systems in ^{85}Rb and ^{87}Rb at natural abundance using the D_2 line and a 10-Torr neon buffer gas was implemented. The Rb cell was kept at 363 K, so the Rb density was $N = 2.4 \times 10^{12}$ cm^{-3}, the optical broadening should be $\gamma_{ab}^{si} = 2\pi \times 334$ MHz, and the hyperfine broadening should be $\gamma_{cb}^{si} = 2\pi \times 16$ kHz. The laser power is given as 100 mW focused in a 2.4-mm diameter spot size, implying that $\Omega_{si} < 2\pi \times 63$ MHz. Based on the experimental results of both the gain and the absorption being roughly equal in height and width with a two-photon HWHM of 125 kHz, we can assume that $\Omega_{s1} = 2\pi \times 34$ and $\Omega_{s2} = 2\pi \times 8$ MHz. The control fields in the experiment are taken such that $\Delta_{s1} = 2\pi \times 15.6$ and $\Delta_{s2} = 2\pi \times 16$ GHz. With an applied pump-field intensity of 1.77 W/cm^2, numerical simulations show that, for a pump field with a bandwidth of about 500 MHz, the population difference for both systems would be close to 1 as needed, with the largest deviation in system 2 with $\sigma_{cc}^{s2} - \sigma_{aa}^{s2} = 0.93$.

The theoretical curve for the resonant RI with these parameters is plotted in Fig. 10. The theory predicts a change in index of $\Delta n = 1.7 \times 10^{-5}$. The theory also shows that there is a background index due to the one-photon feature of $n = 1 + 4 \times 10^{-6}$ since $\xi_{s1} < \gamma_{cb}^{s1}/\gamma_{ab}^{s1}$.

The reported RI change in $\Delta n = 2 \times 10^{-7}$ is 2 orders of magnitude less than what was possible in the experiment [7] due to issues with the cross pumping of the ^{87}Rb and ^{85}Rb populations. As explained in Ref. [7], this could be due to the frequency width of the pump fields being larger than the separation between the hyperfine levels of ^{87}Rb and ^{85}Rb, which would reduce the population difference between

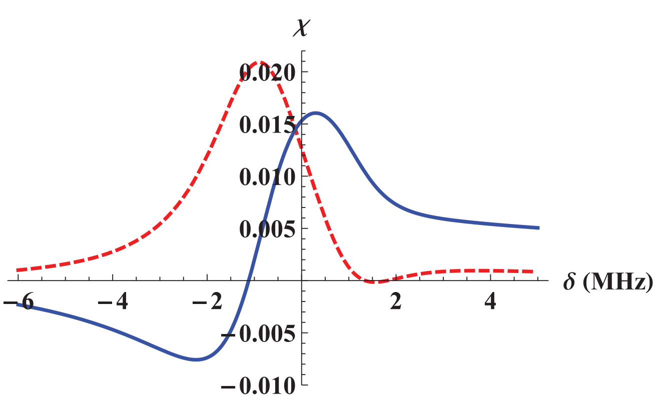

FIG. 8. (Color online) The real (solid) and imaginary (dashed) parts of the susceptibility as a function of the detuning plotted for the scheme without gain and with $\Omega_1 = 2\pi \times 150$ MHz described in the text.

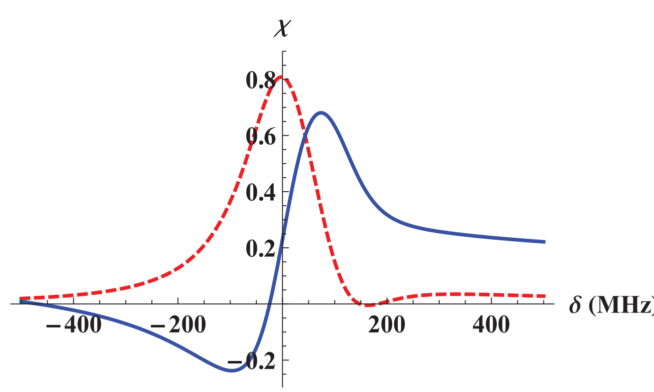

FIG. 9. (Color online) The real (solid) and imaginary (dashed) parts of the susceptibility as a function of the detuning plotted for the scheme with $\Omega_1 = \Omega_2 = 2\pi \times 1.5$ GHz as described in the text.

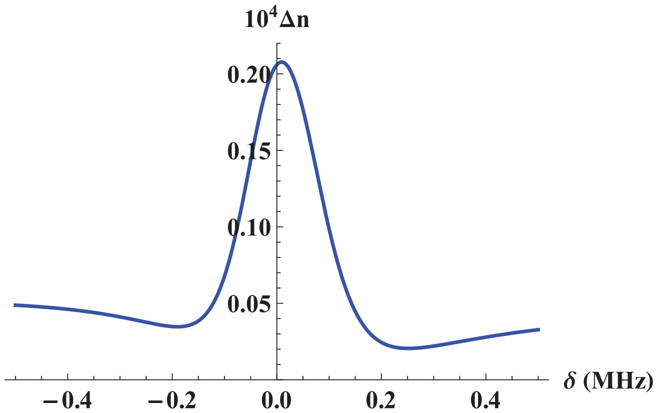

FIG. 10. (Color online) The expected RI enhancement for the experiment described in Ref. [7] plotted as a function of two-photon detuning, using the experimental numbers as reported in the text.

levels $|c_i\rangle$ and $|b_i\rangle$ and, thus, significantly reduce the RI enhancement.

IX. CONCLUSION

We have given a simple model for how to implement RI enhancement without absorption in Rb gas while avoiding any nearby regions of gain. This is performed by implementing a far-detuned Λ system in two different atomic species evenly mixed in a hot gas. In the decaying dressed-state basis, the whole system can be presented as a superposition of two effective two-level schemes with positions, widths, and amplitudes of the resonances determined by the driving fields. It allows for a simple, analytic, and intuitive understanding of the susceptibility for the total system. Thus, a variety of absorption, amplification, and dispersion profiles may easily be engineered. In particular, maximum RI with vanishing absorption results from the simple summation of susceptibilities of the effective absorbing and amplifying two-level schemes whose resonances are positively and negatively tuned with respect to the probe-field frequency. Engineering a larger width for the absorptive resonance allows one to eliminate any amplification region in the vicinity of the enhanced index and vanishing absorption. Proper tuning also allows for the strong increase or decrease in RI under vanishing absorption.

We have shown that, with reasonable beam intensities, this scheme can be implemented in ^{85}Rb and ^{87}Rb at a natural abundance for RI enhancement on the order of $\Delta n \simeq 5 \times 10^{-3}$. This can be performed while maintaining vanishing absorption and with no nearby regions of gain. Potentially higher-resonant RIs with vanishing absorption could be obtained with much stronger beam intensities or in solids (in particular, in rare-earth- and/or transition-metal-ion-doped dielectric crystals or stoichiometric crystals including such ions) [9,16]. The further analysis of the limitations of RI enhancement requires careful studies of optical line self-broadening with an increase in the density and the inclusion of local field effects [17]. Along with the achievement of high RI, it also would be very beneficial for a number of applications to provide for its temporal or spatial modulation. For example, it would allow for the production of controllable photonic structures in a homogeneous medium simply by applying optical fields [18].

ACKNOWLEDGMENTS

This research was supported by NSF Grant No. 0855688. The authors are grateful to Deniz Yavuz for useful discussions.

[1] M. Fleischhauer, C. H. Keitel, M. O. Scully, C. Su, B. T. Ulrich, and S. Y. Zhu, Phys. Rev. A **46**, 1468 (1992).
[2] M. O. Scully, Phys. Rev. Lett. **67**, 1855 (1991).
[3] U. Rathe, M. Fleischhauer, S. Y. Zhu, T. W. Hansch, and M. O. Scully, Phys. Rev. A **47**, 4994 (1993).
[4] M. D. Lukin, S. F. Yelin, A. S. Zibrov, and M. O. Scully, Laser Phys. **9**, 759 (1999).
[5] A. S. Zibrov, M. D. Lukin, L. Hollberg, D. E. Nikonov, M. O. Scully, H. G. Robinson, and V. L. Velichansky, Phys. Rev. Lett. **76**, 3935 (1996).
[6] D. D. Yavuz, Phys. Rev. Lett. **95**, 223601 (2005).
[7] N. A. Proite, B. E. Unks, J. T. Green, and D. D. Yavuz, Phys. Rev. Lett. **101**, 147401 (2008).
[8] P. Anisimov and O. Kocharovskaya, J. Mod. Opt. **55**, 3159 (2008).
[9] C. O'Brien and O. Kocharovskaya, J. Mod. Opt. **56**, 1933 (2009).
[10] E. L. Lewis, Phys. Rep. **58**, 1 (1980).
[11] M. Gorris-Neveux, P. Monnot, M. Fichet, M. Ducloy, R. Barbè, and J. C. Keller, Opt. Commun. **134**, 85 (1997).
[12] J. E. Thomas and W. W. Quivers, Phys. Rev. A **22**, 2115 (1980).
[13] M. Shuker, O. Firstenberg, Y. Sagi, A. Ben-kish, N. Davidson, and A. Ron, Phys. Rev. A **78**, 063818 (2008).
[14] M. D. Rotondaro and G. P. Perram, J. Quant. Spectrosc. Radiat. Transfer **57**, 497 (1997).
[15] I. Novikova, A. V. Gorshkov, D. F. Phillips, Y. Xiao, M. Klein, and R. L. Walsworth, Proc. SPIE **6482**, 64820M (2007).
[16] M. E. Crenshaw, C. M. Bowden, and M. O. Scully, J. Mod. Opt. **50**, 2551 (2003).
[17] J. P. Dowling and C. M. Bowden, Phys. Rev. Lett. **70**, 1421 (1993).
[18] C. O'Brien and O. Kocharovskaya, Phys. Rev. Lett. **107**, 137401 (2011).